Theoretical analysis of the modal dispersion induced by stresses in a multimode plastic optical fibre

J.Zubia
J.Arrue

Indexing terms: Fibre optics, Modal dispersion, Plastic optical fibre, Stress analysis, Birefringence

Abstract: The authors have analysed how bending, torsion and tensile stresses affect the dispersion and polarisation in a plastic optical fibre. This respectively becomes locally uniaxial and inhomogeneous, biaxial and inhomogeneous, and uniaxial and homogeneous, with little variation in the dispersion. The polarisation changes rapidly and the induced anisotropy is of the order of that produced in the manufacturing process.

1 Introduction

Although, until a few years ago, most of the studies were focused on conventional glass optical fibres, the recently discovered plastic optical fibre (POF) has attracted a lot of attention. Despite its higher attenuation, a POF is easier to handle and cheaper than a glass fibre [1–3], serving for small distance links, even at very high data rates, with the new graded-index POFs [4].

For these reasons, many efforts have been devoted to the study of properties of POFs. However, some minor aspects as, for example, the photoelastic or stress-optical effect, still require a systematic study. This paper analyses the effects of different stresses on the dispersion and is based on our previous work on the torsion induced optical effect [5].

2 Theoretical background

The theoretical analysis in this Section is based on some essential assumptions about the structure and properties of a POF. We suppose that an undisturbed POF is an isotropic, transparent and homogeneous medium, so we do not consider the cladding. It is obvious that the production process induces anisotropy [6], as we show later, with some minor differences between the optical behaviour along the axis of the fibre and that along the axis perpendicular to it. However, these differences are neglected at this stage.

As is well known, the stress can be characterised by a symmetric second-rank tensor $[\sigma]$ with six independent components σ_i (i = 1, ..., 6). We use the common contracted notation [7] to number the elements of $[\sigma]$. The photoelastic or stress-optical effect is then described, up to first order in the stresses, by the relation:

$$\Delta \mathbf{B}_i = \mathbf{q}_{ij}\sigma_j \tag{1}$$

where ΔB_i (i = 1, ..., 6) is a symmetric second-rank tensor that represents the changes of coefficients in the optical indicatrix or index ellipsoid under the action of applied stresses. The stress-optical tensor, q_{ij}, is a fourth-rank tensor with 36 components (i, j = 1, ..., 6).

When the symmetry of an isotropic medium such as a POF is taken into account, the number of independent elements in the tensor q_{ij} is finally reduced to two different ones, $\mathbf{q}_{11}$ and $\mathbf{q}_{12}$, arranged as:

$$[\mathbf{q}] = \begin{bmatrix} q_{11} & q_{12} & q_{12} & 0 & 0 & 0 \\ q_{12} & q_{11} & q_{12} & 0 & 0 & 0 \\ q_{12} & q_{12} & q_{11} & 0 & 0 & 0 \\ 0 & 0 & 0 & q_{11}-q_{12} & 0 & 0 \\ 0 & 0 & 0 & 0 & q_{11}-q_{12} & 0 \\ 0 & 0 & 0 & 0 & 0 & q_{11}-q_{12} \end{bmatrix} \tag{2}$$

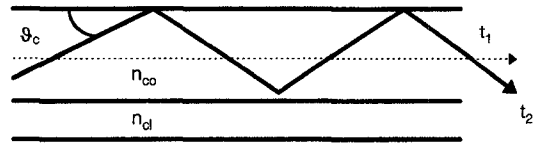

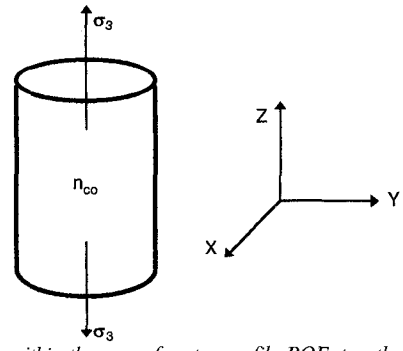

Fig. 1 *Zigzag path within the core of a step-profile POF, together with the geometry and reference system for a POF subjected to a tensile stress*

In the following Sections, we calculate the change in the modal dispersion originated by each type of stress. Modal dispersion is defined as the difference between the maximum and minimum ray transit times, which, in Fig. 1, are the times corresponding to the ray

© IEE, 1997

IEE Proceedings online no. 19971561
Paper first received 3rd February and in revised form 29th July 1997

The authors are with the Departamento de Electrónica y Telecomunicaciones, ETSII y IT, University of the Basque Country, Alameda de Urquijo s/n, 48013–Bilbao, Spain

making an angle θ_c with the fibre axis and to the ray parallel to the axis. The complementary critical angle θ_c is given by $\theta_c = \cos^{-1}(n_{cl}/n_{co})$, where n_{cl} and n_{co} are the cladding and core refractive indices, respectively.

2.1 Effect of a uniaxial stress

First, we analyse the effect of a tensile stress applied parallel to the fibre axis. As a consequence, the indices of refraction increase by [5]:

$$\Delta n_x = \Delta n_y = -n_{co}^3 q_{12}\sigma_3/2 \quad \Delta n_z = -n_{co}^3 q_{11}\sigma_3/2 \tag{3}$$

which means that the POF becomes birefringent, with the principal axes located parallel and perpendicular to the direction of the tensile stress (Fig. 1). As this tensile stress is usually present in any POF-production process, POFs are slightly birefringent, with a preferred direction (the optic axis) along the fibre axis. Even if tensile stresses were absent, the temperature changes along the fibre in the production process would give rise to a similar effect [6].

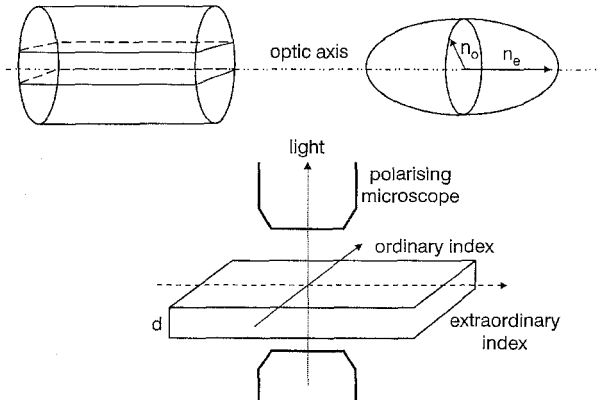

Fig. 2 *Geometry of sample used to measure birefringence*
$d = 376\mu m$

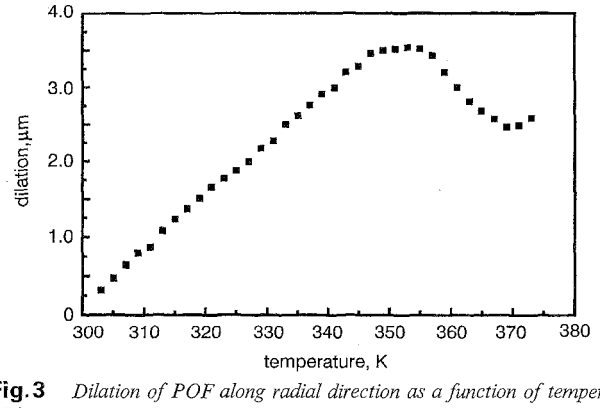

Fig. 3 *Dilation of POF along radial direction as a function of temperature*

The birefringence of a commercial PMMA POF (Eska Extra from Mitsubishi Rayon) was determined experimentally. For this purpose, a small section of POF was cut and polished isotropically in the axial direction to obtain a perfect parallelogram, as is shown in Fig. 2. The sample was introduced in a Mettler hot stage to control the temperature, and the hot stage was placed between crossed polarisers in an Olympus polarising microscope. To measure the birefringence we used a Berek compensator. This procedure allows us to obtain the variation of the product Δnd with temperature. d stands for the sample thickness. To deduce the behaviour of the birefringence, we also measured the dilation of the POF in the transverse direction by means of a Perkin-Elmer thermomechanical analyser TMA 500. The increase in length along the radial direction $\Delta d(T)$ is shown in Fig. 3 and the resulting birefringence in Fig. 4. The drop observed in the dilation curve is caused by the changes that the polymer experiences close to the glass transition point. The birefringence was measured for several POF slabs to ascertain that the anisotropy was intrinsic and not due to the polishing process. No noticeable differences in the birefringence values were obtained. It is seen that the induced birefringence is negative, i.e. $n_o > n_e$, and decreases monotonicaly as we approach the glass transition temperature. At 393K the birefringence was very small. The reason for this behaviour lies in the growing disorder, which leads to an increasing symmetry, and so to a reduced birefringence. In our experiments, the size of the light spot was around $1\,mm^2$, which means that the measured birefringence represents an average value.

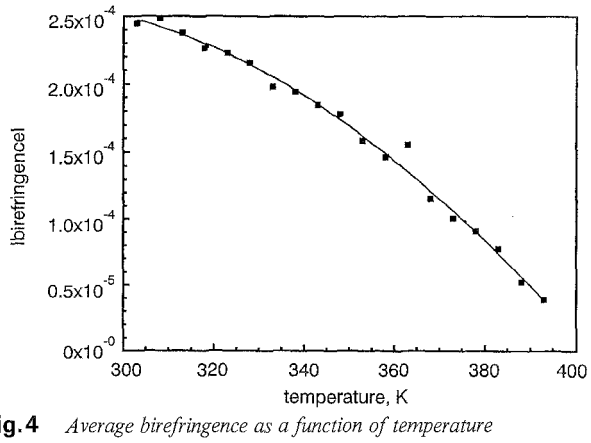

Fig. 4 *Average birefringence as a function of temperature*

To calculate the effect of a uniaxial stress on the dispersion, we consider the change in the maximum and minimum meridional ray transit times. The transit time for a ray travelling parallel to the fibre axis is minimum and is modified by a uniaxial stress according to the expression $\Delta t_{min}^u = \Delta(Ln_{co})/c$, as follows:

$$\begin{aligned}\Delta t_{min}^u &= \Delta(Ln_{co})/c \\ &= n_{co}\Delta L/c + L\Delta n_{co}/c \\ &= Ln_{co}\sigma_3/cE - Ln_{co}^3 q_{12}\sigma_3/2c \end{aligned} \tag{4}$$

$$\Delta t_{min}^u = \frac{Ln_{co}\sigma_3}{cE}\left(1 - \frac{n_{co}^2 q_{12}}{2}E\right) \tag{5}$$

L being the total fibre length and E being Young's modulus. This expression is independent of the ray polarisation.

The transit time for a ray propagating at an angle θ_c with the fibre axis is maximum and varies in a similar way. However, contrary to what happens with isotropic fibres, the refractive index depends on the concrete ray direction. The ordinary ray propagates with an index of refraction equal to $n_o^u = n_{co}(1 - n_{co}^2\sigma_3 q_{12}/2)$, independently of the angle θ_c. For the extraordinary ray, the index of refraction can be inferred from the following well known formula [8]:

$$\frac{1}{n_e^{u2}(\theta_c)} = \frac{\cos^2\theta_c}{[n_{co}(1 - n_{co}^2\sigma_3 q_{12}/2)]^2} + \frac{\sin^2\theta_c}{[n_{co}(1 - n_{co}^2\sigma_3 q_{11}/2)]^2} \tag{6}$$

which, to a good approximation, yields

$$n_e^u = n_{co}[1 - n_{co}^2\sigma_3(q_{11}\sin^2\theta_c + q_{12}\cos^2\theta_c)/2] \quad (7)$$

Then, the correction to the maximum ray transit time turns out to be [9]:

$$\Delta t_{max,i}^u = \Delta(Ln_i\sec\theta_c)/c$$
$$= n_i\sec\theta_c\Delta L/c + L\sec\theta_c\Delta n_i/c + Ln_i\Delta\sec\theta_c/c \quad (8)$$

where n_i stands for both the ordinary and extraordinary refractive indices, and

$$\Delta\sec\theta_c = \cos\theta_c(2\Delta r_{core}\tan\theta_c - \Delta L\tan^2\theta_c)/L \quad (9)$$

where r_{core} stands for the core radius and σ for the Poisson ratio and $\Delta r_{core} = -r_{core}\sigma\Delta L/L$.

$$\Delta n_o = -n_{co}^3\sigma_3 q_{12}/2$$

and

$$\Delta n_e = -n_{co}^3\sigma_3(q_{11}\sin^2\theta_c + q_{12}\cos^2\theta_c)/2 \quad (10)$$

Introducing eqns. 9 and 10 into eqn. 8, we obtain:

$$\Delta t_{max,o}^u = Ln_{co}\sigma_3[\sec\theta_c(1 - En_{co}^2 q_{12}/2) - \sin\theta_c(2r_{core}\sigma/L + \tan\theta_c)]/cE \quad (11)$$

$$\Delta t_{max,e}^u = Ln_{co}\sigma_3 \times[\sec\theta_c(1-En_{co}^2(q_{11}\sin^2\theta_c+q_{12}\cos^2\theta_c)/2) - \sin\theta_c(2r_{core}\sigma/L + \tan\theta_c)]/cE \quad (12)$$

All this allows us to calculate the dispersion. This will be $\Delta t_{max,i}^u - \Delta t_{min,i}^u$, where the subindex i accounts for the polarisation direction, which yields:

$$\Delta t_o^u = Ln_{co}\sigma_3[(\sec\theta_c - 1)(1 - En_{co}^2 q_{12}/2) - \sin\theta_c(2r_{core}\sigma/L + \tan\theta_c)]/cE \quad (13)$$

$$\Delta t_e^u = Ln_{co}\sigma_3 \times [\sec\theta_c(1 - En_{co}^2(q_{11}\sin^2\theta_c + q_{12}\cos^2\theta_c)/2) - \sin\theta_c(2r_{core}\sigma/L + \tan\theta_c) - 1 + En_{co}^2 q_{12}/2]/cE \quad (14)$$

2.2 Effect of fibre bending

In this Section, we calculate the new refractive indices and the principal axes of the index ellipsoid when a fibre is bent in the XY-plane, as shown in Fig. 5. Contrary to what is observed in single-mode fibres, bending a POF produces a birefringence that varies linearly with the distance to the neutral line [10].

2.2.1 Principal refractive indices in a bent POF: Fig. 5 shows the reference system chosen for our analysis of circular bends. Owing to the symmetry of our problem, the stress tensor is calculated in cylindrical co-ordinates (i.e. (ρ, φ, z)), and the only nonzero component turns out to be σ_φ [11]. If R denotes the bend radius, this stress component can be written as

$$\sigma_\varphi = E(\rho - R)/R \quad (15)$$

Changing to Cartesian co-ordinates in order to use eqn. 1, the new indicatrix is found to be:

$$\left(\frac{1}{n_{co}^2} + q_{11}\sigma_\varphi\sin^2\varphi + q_{12}\sigma_\varphi\cos^2\varphi\right)x^2 + \left(\frac{1}{n_{co}^2} + q_{12}\sigma_\varphi\sin^2\varphi + q_{11}\sigma_\varphi\cos^2\varphi\right)y^2 + \left(\frac{1}{n_{co}^2} + q_{12}\sigma_\varphi\right)z^2 + 2xy(q_{11}-q_{12})\sigma_\varphi\cos\varphi\cdot\sin\varphi = 1 \quad (16)$$

The next step is finding the directions and magnitudes of the principal axes of the index ellipsoid. Table 1 shows the results. From the eigenvalues of the matrix **[B]**, we can write the corrections to the index of refraction as $\Delta n_i = -n_{co}^3\Delta B_i/2$.

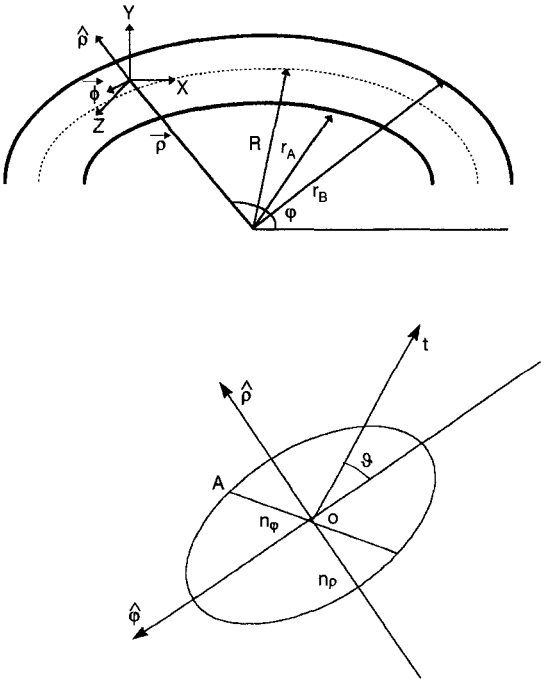

Fig. 5 *Geometry and reference system for a bent POF, together with the section of the index ellipsoid on the plane of the bend*
$\hat{t}$ stands for the direction of the ray under consideration. n_ρ and n_φ are the refractive indices along the polar directions $\hat{\rho}$ and $\hat{\varphi}$.

2.2.2 Index of refraction along an arbitrary direction in the plane of the bend: In this Section, we consider the propagation of rays along some arbitrary direction in the fibre. For this purpose, we make use of the index ellipsoid referred to its principal axes. Let us analyse a ray $\hat{t}$ propagating at an angle θ with the optic axis $\hat{\varphi}$ (Fig. 5). There are two allowed polarisation directions, with different refractive indices. The first of these two waves, which is polarised along

Table 1: Principal axis vectors of index ellipsoid and corresponding indices of refraction for POF subjected to bending stress

Eigenvectors	V_1	V_2	V_3
Components	(0, 0, 1)	(cos φ,sinφ,0)	(−sinφ,cosφ,0)
Refractive index	$n_z = n_{co}(1-(n_{co}^2/2)q_{12}\sigma_\varphi)$	$n_\rho = n_{co}(1-(n_{co}^2/2)q_{12}\sigma_\varphi)$	$n_\varphi = n_{co}(1-(n_{co}^2/2)q_{11}\sigma_\varphi)$

φ is the angle with the polar axis and σ_φ is the bending stress

the z-direction, is the ordinary wave and has an index of refraction $n^b{}_o$:

$$n_o^b = n_z = n_{co}(1 - n_{co}^2 q_{12}\sigma_\varphi/2) \tag{17}$$

The refractive index of the extraordinary ray, $n^b{}_e$, varies with θ according to the expression:

$$\frac{1}{n_e^{b2}(\theta)} = \frac{\cos^2\theta}{n_\rho^2} + \frac{\sin^2\theta}{n_\varphi^2}$$

$$n_e^b(\theta) \approx n_{co}(1 - n_{co}^2\sigma_\varphi(q_{12}\cos^2\theta + q_{11}\sin^2\theta)/2) \tag{18}$$

In the last two equations, we have supposed that the corrections are much less than unity. Depending on the sign of σ_φ, the ordinary and extraordinary rays will travel faster or slower than in the case of an undisturbed fibre. This effect becomes more important as we withdraw from the neutral line.

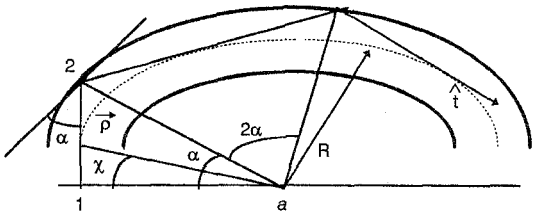

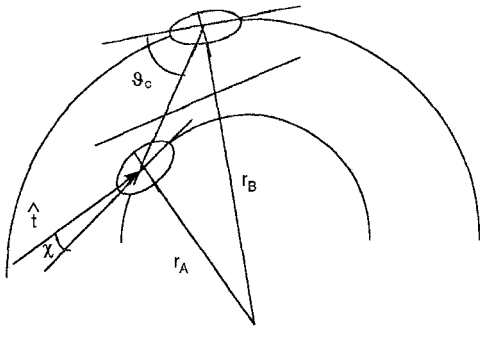

b

Fig. 6 *Geometry of a bent optical fibre*
a Meridional ray entering the bend tangentially to the fibre axis
b Meridional ray at an angle θ_c with the outer surface

2.2.3 Correction to the dispersion when bending a POF:

A rigorous analysis would involve the calculation of an expression for the transit time of skew rays, which generally depends on the invariants β and l [12]. However, if the bend radius is not too small, transit times of skew rays are expected to be identical to those of meridional rays. Consequently, to calculate the dispersion, we will compare two rays in the plane of the bend: that entering the bend along the fibre axis and that making an initial angle θ_c with the fibre axis, as shown in Fig. 6. The correction to the time spread can be calculated as:

$$\Delta t_o^b = \frac{ELn_{co}^3 q_{12}}{2\alpha \cdot c}\left[\tan\alpha\left(1 - \frac{1}{2\cos\alpha}\right) - \frac{1}{2}\ln\tan\left(\frac{\alpha}{2} + \frac{\pi}{4}\right)\right] \tag{19}$$

$$\Delta t_e^b = \frac{ELn_{co}^3}{2\alpha \cdot c}\left[q_{11}\tan\alpha\left(1 - \frac{1}{2\cos\alpha}\right) - \left(q_{12} - \frac{q_{11}}{2}\right)\ln\tan\left(\frac{\alpha}{2} + \frac{\pi}{4}\right) + (q_{12} - q_{11})\alpha\right] \tag{20}$$

The procedure to reach this result can be summarised as follows:

First, we calculate the transit times for the ordinary and extraordinary rays initially parallel to the fibre axis. To do so, we must integrate to obtain the ray transit time t_{2i} between two reflection points:

$$dt = \frac{n}{c}ds = \frac{Rn(\chi)d\chi}{c\cos^2\chi}$$

$$t_{2i} = \frac{2R}{c}\int_0^\alpha \frac{n(\chi)d\chi}{\cos^2\chi} \tag{21}$$

Then, we repeat the method for the corresponding rays entering the bend at an angle θ_c. From Fig. 6, it is easy to see that $\cos\chi = r_B/r_A\cos\vartheta_c$. If $R >> r_B - r_A$, $\cos\chi \approx \cos\vartheta_c$. In such a case, we can consider the angle between the ray $\hat{\mathbf{t}}$ and the principal axis $\hat{\varphi}$ of the index ellipsoid as constant and equal to θ_c. With all these assumptions, we can compute the extraordinary ray transit time between two consecutive reflections:

$$t_{2ie} = \frac{1}{c}\int_{r_A}^{r_B} n_e(\theta_c)ds$$

$$t_{2ie} = \frac{1}{c}\int_{r_A}^{r_B} n_{co}\left[1 - \frac{n_{co}^2\sigma_\varphi}{2}(q_{12}\cos^2\theta_c + q_{11}\sin^2\theta_c)\right]ds \tag{22}$$

For the ordinary ray, we proceed in a similar way. The stress has no effect on that ray transit time.

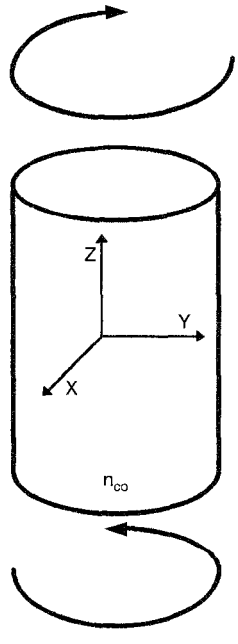

Fig. 7 *Torsion of POF when pure shear forces are applied at both ends of the fibre*
The arrows indicate the directions of the forces applied to the POF. In the Figure, the reference system used in the text is also shown.

2.3 Effect of fibre torsion

The geometry of the problem is illustrated in Fig. 7. Shear forces are applied at both ends of the fibre

Table 2: Principal axis vectors of index ellipsoid and corresponding indices of refraction for POF subjected to torsion stress

Eigenvectors	V_1	V_2	V_3
Components	$(\cos\vartheta, \sin\vartheta, 0)$	$(1/\sqrt{2})(\sin\vartheta, -\cos\vartheta, 1)$	$(1/\sqrt{2})(\sin\vartheta, -\cos\vartheta, -1)$
Refractive index	n_{co}	$n_{co}(1-n_{co}^2(q_{11}-q12)\mu\tau r/2)$	$n_{co}(1+n_{co}^2(q_{11}-q12)\mu\tau r/2)$

r and θ stand for the usual polar co-ordinates: $r = (x^2 + y^2)^{1/2}$ and $\theta = \tan^{-1}(y/x)$

Table 3: Summary of results of corrections to the time spread originated by different stresses

Stress	Correction to the time spread
Uniaxial	
Ordinary	$\Delta t_o^u = Ln_{co}\sigma_3[(\sec\theta_c-1)(1-En_{co}^2q_{12}/2)-\sin\theta_c(2r_{core}\sigma/L+\tan\theta_c)]/cE$
Extraordinary	$\Delta t_e^u = Ln_{co}\sigma_3[(\sec\theta_c(1-En_{co}^2(q_{11}\sin^2\theta_c+q_{12}\cos^2\theta_c)/2)-\sin\theta_c(2r_{core}\sigma/L+\tan\theta_c)-1+LEn_{co}^2q_{12}/2]/cE$
Bending	
Ordinary	$\Delta t_o^b = (ELn_{co}^3q_{12}/2c\alpha)[\tan\alpha(1-1/2\cos\alpha)-(1/2)\ln\tan(\alpha/2+\pi/4)]$
Extraordinary	$\Delta t_e^b = (ELn_{co}^3/2c\alpha)[q_{11}\tan\alpha(1-1/2\cos\alpha)-(q_{12}-(q_{11}/2)\ln\tan(\alpha/2+\pi/4)+(q_{12}-q_{11})\alpha]$
Torsion	
Ordinary (–)	$\Delta\tau_-^2 = (-n_{co}^3L\cdot q_{44}\mu\tau r_{core}\tan\vartheta_d/4c)$
Extraordinary (+)	$\Delta\tau_+^2 = (+n_{co}^3L\cdot q_{44}\mu\tau r_{core}\tan\vartheta_d/4c)$

For each type of stress, two different corrections, corresponding to different polarisation directions, have been calculated

section, to produce a torsion on it. In this situation, the components of the stress tensor will be [11]:

$$\sigma_1 = \sigma_2 = \sigma_3 = \sigma_6 = 0$$
$$\sigma_4 = \mu\tau x$$
$$\sigma_5 = -\mu\tau y \tag{23}$$

where τ is the torsion angle, defined as $\tau = d\varphi/dz$, and μ is the stiffness constant. Introducing these components in eqn. 1, we find that the refractive index depends both on the position and on the ray polarisation. The eigenvectors and their corresponding eigenvalues are given in Table 2. It can be seen that the z-direction is no longer an optic axis of the medium. However, along the fibre axis $r = 0$, the index ellipsoid is spherical and independent of polarisation, which means that the minimum ray transit time, t_{min}^{τ}, is not affected by the torsion. This result is a consequence of the fact that the stress on the fibre axis is null ($\sigma_i = 0$). As the anisotropy for any other direction, say $\hat{\mathbf{t}}$, is not null, we have to calculate the corresponding refractive index, n_t, by means of Fresnel's ray-equation:

$$\frac{t_{V_1}^2}{n_t^2 - n_{V_1}^2} + \frac{t_{V_2}^2}{n_t^2 - n_{V_2}^2} + \frac{t_{V_3}^2}{n_t^2 - n_{V_3}^2} = 0 \tag{24}$$

For the ray propagating at an angle θ_c shown in Fig. 1, in the reference system formed by the principal eigenvectors ($\hat{\mathbf{t}} = (\sin\vartheta_c, 1/\sqrt{2}\cos\vartheta_c, 1/\sqrt{2}\cos\theta_c)$) and choosing the eigenvector $\mathbf{V}_1$ to be in the plane of the meridional ray, eqn. 24 yields:

$$\frac{\sin^2\theta_c}{n_t^2 - n_{co}^2} + \frac{\frac{1}{2}\cos^2\theta_c}{n_t^2 - n_{co}^2(1-f)^2} + \frac{\frac{1}{2}\cos^2\theta_c}{n_t^2 - n_{co}^2(1+f)^2} = 0 \tag{25}$$

where $f = n_{co}^2(q_{11} - q_{12})\mu\tau r/2$. From this equation, we can deduce the value of n_t:

$$n_t = n_{co}\sqrt{1 \pm 2f\sin\theta_c} \tag{26}$$

neglecting second-order corrections in the anisotropy and considering that the energy propagates in the direction of the wave normal. Now, if we calculate the radius r_{tp} at which each ray would touch the turning-point caustic, we can see that r_{tp} is typically much larger than the core radius (remembering that, for a typical POF, $n_{co} = 1.492$, $n_{cl} = 1.417$ and $r_{core} = 0.5\ 10^{-3}$m), so ray trajectories can be considered as straight:

$$r_{tp} = \frac{(n_{co}^2 - n_{cl}^2)}{n_{co}^4(q_{11} - q_{12})\mu\tau\sin\theta_c} \gg r_{core} \tag{27}$$

The difference between the maximum and minimum ray transit times gives the time spread. As we have already pointed out, $t_{min}^{\tau} = n_{co}L/c$. On the other hand, t_{max}^{τ} can be inferred as follows. The time between two reflections will be:

$$\begin{aligned} t_{max}^{\tau} &= \int_0^{r^{core}} \frac{n(r)dr}{c\sin\theta_c} \\ &= \frac{1}{c\sin\theta_c}\int_0^{r^{core}} n_{co}(1 \pm 2f\sin\theta_c)^{1/2}dr \\ t_{max}^{\tau} &\approx \frac{1}{c\sin\theta_c}\int_0^{r^{core}} n_{co}(1 \pm q_{44}n_{co}^2\tau\mu r\sin\theta_c/2)dr \\ &= \frac{n_{co}r_{core}}{c\sin\theta_c}(1 \pm q_{44}n_{co}^2\tau\mu r_{core}\sin\theta_c/4) \end{aligned} \tag{28}$$

This is the time that a ray takes to travel a distance $z = r_{core}/\tan\theta_c$, so for a distance L we have ($q_{44} = q_{11} - q_{12}$):

$$\begin{aligned} t_{max}^{\tau} &= \frac{n_{co}r_{core}}{c\sin\theta_c}(1 \pm n_{co}^2q_{44}\mu\tau r_{core}\sin\theta_c/4)\frac{L}{z} \\ &= \frac{n_{co}L}{c\cos\theta_c}(1 \pm n_{co}^2q_{44}\mu\tau r_{core}\sin\theta_c/4) \end{aligned} \tag{29}$$

Hence, the time spread is

$$\Delta t_{\pm}^{\tau} = \frac{n_{co}L}{c}\left(\frac{1 \pm n_{co}^2q_{44}\mu\tau r_{core}\sin\theta_c/4}{\cos\theta_c} - 1\right) \tag{30}$$

The double sign corresponds to two different polarisation directions (Table 3).

3 Discussion

Stresses affect both the refractive index and the dispersion. With regard to uniaxial or tensile stress, one effect is the appearance of a linear birefringence. This is given by:

$$\Delta n^u = n_e^u - n_o^u = -n_{co}^3 \sigma_3 (q_{12} \cos^2\theta + q_{11} \sin^2\theta)/2 \quad (31)$$

It is, therefore, independent of the point considered and directly proportional to the magnitude of the stress.

Calculating the birefringence induced by a moderate stress in a fibre of length L, we know that the induced anisotropy is maximum for a ray propagating at an angle θ_c with the fibre axis, and the corresponding optical phase shift is

$$\delta\varphi = \frac{-\pi n_{co}^3 \sigma_3 (q_{12} \cos^2\theta_c + q_{11} \sin^2\theta_c)}{\lambda \cos\theta_c} \quad (32)$$

This means that the polarisation state will repeat itself for each beat length L_p^u, defined as

$$L_p^u = \frac{2\pi}{\delta\varphi} = \left| \frac{2\lambda \cos\theta_c}{n_{co}^3 \sigma_3 (q_{12} \cos^2\theta_c + q_{11} \sin^2\theta_c)} \right| \quad (33)$$

This is of the order of 10^{-3}m for typical values of these parameters (Table 4), so uniaxial stresses have a great influence on the polarisation state. As we approach the glass transition temperature T_g, this effect is expected to be more important [13, 14]. As a moderate tensile stress is also applied in any POF production process, we measured the intrinsic optical anisotropy of a commercial POF to obtain a rough estimation of the birefringence. When the measured optical anisotropy (Fig. 4) is used to calculate L_p^u, the same order of magnitude is obtained.

Regarding the variation of the time spread, a tensile stress originates a decrease in the ray transit times, to a greater extent as the angle with the optical-fibre axis increases. Each point of the curve in Fig. 8 represents the correction that has to be applied to each original ray transit time, which is given by the x co-ordinate, assuming that we begin to count the time when the first ray arrives. The corrections are of the order of the dispersion in a graded-index POF (78ps in 25ns) [4, 15]. To calculate this curve, we have neglected random variations in the fibre diameter during the manufacturing process [13]. Although the effect of a tensile stress on the dispersion is negligible, the same does not occur with the polarisation direction, which changes very rapidly.

A bending stress makes the POF locally uniaxial, with the revolution axis orientated tangentially to the fibre symmetry axis. The directions of the principal axes depend on the polar angle, but not on the co-ordinates ρ or z. The induced anisotropy, which is directly proportional to the distance to the neutral line and inversely proportional to the bend radius R, is given by:

$$\begin{aligned} \Delta n^b &= n_e^b - n_o^b \\ &= \frac{n_{co}^3}{2} \sigma_\varphi (q_{12} - q_{11}) \sin^2\theta \\ &= \frac{-n_{co}^3}{2} \sigma_\varphi q_{44} \sin^2\theta \\ &= \frac{n_{co}^3 (R-\rho) E}{2R} q_{44} \sin^2\theta \end{aligned} \quad (34)$$

This behaviour is opposite to that observed in single mode fibres, in which the bending birefringence varies as the square of r_{core}/R [10].

A torsion stress makes the POF slightly biaxial. The correction term for the refractive indices along two of the principal axes of the index ellipsoid, given by $n_{co}^3(q_{11} - q_{12})\mu\tau r/2$, is much less than unity ($10^{-4} - 10^{-5}$) and only depends on the radial co-ordinate. Along the fibre axis ($r = 0$), the index ellipsoid becomes a sphere, so this direction will be isotropic. Going far away from the fibre axis, the index ellipsoid becomes more and more asymmetric and the fibre more birefringent. When the wavelength is of the order of the pitch of the twist, a torsion stress leads to a circular birefringence proportional to the twist [10]. In our case, however, the pitch considered in our calculation (one turn per metre) is much greater than the light source wavelength. Therefore, circularly polarised waves are not normal modes of the twisted fibre.

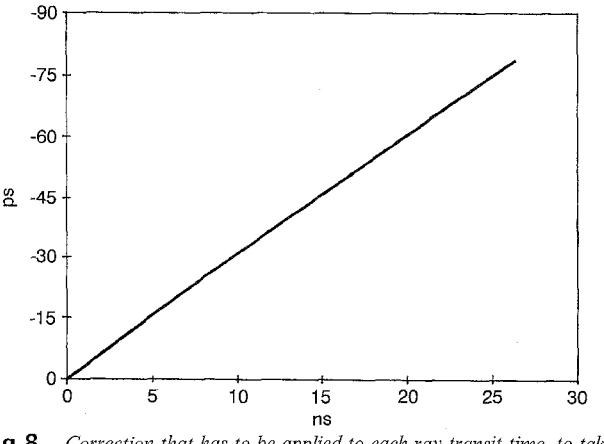

Fig. 8 *Correction that has to be applied to each ray transit time, to take into account the birefringence induced by a tensile stress, against the ray transit time in the absence of stresses*

The beat length resultant with each stress is very small, especially with bending stresses (Table 4), which

Table 4: Expression of beat length, its value and magnitude of correction to dispersion with tensile, bending and torsion stresses

	Tensile	Bending	Torsion
Beat Length	$L_p^u = \lvert(2\lambda\cos\vartheta_c/n_{co}^3\sigma_3(q_{11}\sin^2\vartheta_c + q_{12}\cos^2\vartheta_c))\rvert$	$L_p^b = \lvert(2\lambda/n_{co}^3 q_{44}\sigma_\varphi \sin^2\vartheta_c)\rvert$	$L_p^\tau = \lvert(4\lambda/n_{co}^3 q_{44}\mu\tau r_{core}\tan\vartheta_c)\rvert$
Beat Length	10^{-2}m	10^{-3}m	10^{-1}–10^{-2}m
Correction to time spread	–78ps	–0.064ps	±0.31ps

The values of the correction to the dispersion have been calculated for the ordinary ray per 100 m, using the following typical parameters: $\sigma_3 = 10^7$ N/m², $\lambda = 600$ nm, $n_{co} = 1.492$, $q_{11} \approx q_{12} \approx q_{44} \approx 10^{-12}$ m²/N, R = 10^{-2} m, $r_{core} = 0.5\ 10^{-3}$ m, $\mu = 1.1\ 10^9$ N/m², $\sigma = 0.4$, $\tau = 2\pi$ rad/m, $E = 3.2\ 10^9$ N/m² and, finally, $\theta_c = 18.24° = 0.318$ rad

shows that the polarisation state changes rapidly. The same does not happen with the dispersion correction term, which is negligible in all cases (Table 4, Figs. 8 and 9). Fig. 9 is the counterpart to Fig. 8 for bending and torsion stresses. In this case, as in Fig. 8, the ordinary and extraordinary rays both give rise to the same curve, as we have considered $q_{11} = q_{12}$. The corrections to the time spread for bending and torsion stresses are even smaller than that for tensile stresses.

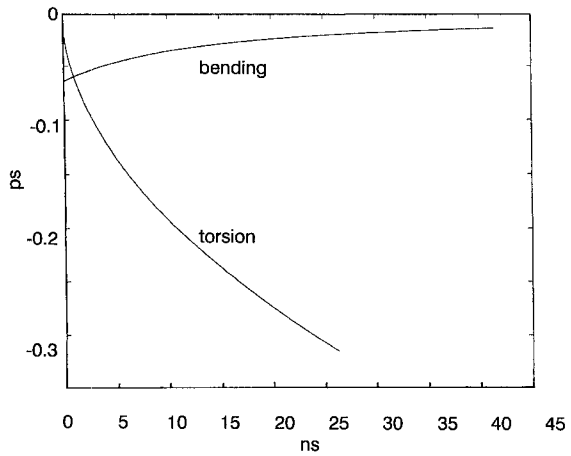

Fig.9 *Correction that has to be applied to each ray transit time, to take into account the birefringence induced by bending and torsion stresses, against the ray transit time in the absence of stresses*

With the above results and the value of Young's modulus, we can infer indirectly the approximate values of the photoelastic coefficients q_{11} and q_{12} by measuring L_p^{u} and L_p^{r}. The approximation is good, because the change δ in the polarisation state is much more than that provoked by the reflections at the core-cladding interface along the same length of fibre ($\approx 10^{-2}$ or 10^{-3}m). δ is given by [8]:

$$\tan\frac{\delta}{2} = \frac{\sin\theta_i\sqrt{\cos^2\theta_i - \frac{n_{cl}^2}{n_{co}^2}}}{\cos^2\theta_i} \qquad (35)$$

which yields a phase change of only 0.1 degrees for the most tilted bound rays, for which the distance between two total-internal-reflection points can be calculated as $2r_{core}/\tan\theta_c = 6.1 \times 10^{-3}$m.

To some extent, another factor that could hide these results is the intrinsic anisotropy of the refractive index. POFs are manufactured by means of a melt spinning process. At the final step of the production process, POFs are drawn out from the nozzle at a controlled diameter, by regulating the polymer temperature, the drawing velocity and other factors [1]. The magnitude of the intrinsic anisotropy induced at this stage turns out to be around $10^{-4} - 10^{-5}$ [13, 15], which is of the order of the stress-induced anisotropy. This value coincides with our measurements.

Finally, we note that the results obtained here do not vary significantly when the mechanical properties of the cladding and jacket are taken into account. When doing so, their effect is expected to change the value of E and μ, but not the qualitative dependence of the dispersion and beat length on these parameters [5].

4 Conclusions

We have analysed the optical effects induced by three different types of stresses. A uniaxial stress makes the isotropic POF uniaxial with its optic axis parallel to the fibre axis. On the other hand, bending and torsion stresses convert the fibre into an inhomogeneous medium, because the refractive index depends on the position as well as on the direction of the ray path through the POF. While, as a result of a bending stress, the fibre becomes locally uniaxial, twisting a fibre produces a biaxial medium. All in all, the main conclusion is that these stresses have no noticeable effect on the modal dispersion, although they could yield a significant contribution to the dispersion of a graded index POF. However, bending and tensile stresses make the polarisation state vary very rapidly. In any case, the magnitude of the induced anisotropy for moderate stresses results is similar to intrinsic manufacturing anisotropy.

5 Acknowledgment

This work is supported by the Departamento de Industria del Gobierno Vasco under project UE96/38.

6 References

1 KAINO, T., and KATAYAMA, K.: 'Polymer for optoelectronics', *Polym. Eng. Sci.*, 1989, **29**, pp. 1209–1214
2 HANSON, D.: 'Wiring with plastic', *IEEE LTS*, 1992, **3**, (1), pp. 34–39
3 KAINO, T.: 'Polymers for lightwave and integrated optics' (Marcel Dekker Inc., New York, 1992)
4 ISHIGURE, T., NIHEI, E., KOIKE, Y., FORBES, C.E., LANIEVE, L., STRAFF, R., and DECKERS, H.A.: 'Large core, high-bandwith polymer optical fiber for near infrared use', *IEEE Photonics Technol. Lett.*, 1995, **7**, pp. 403–405
5 ZUBIA, J., ARRUE, J., and MENDIOROZ, A.: 'Theoretical analysis of the torsion-induced optical effect in a plastic optical fibre', *Opt. Fiber Technol.*, 1997, **3**, (2), pp. 162–167
6 MILLER, S.A., and KAMINOW, I.P.: 'Optical fiber communications II' (Academy Press, San Diego, 1988)
7 NYE, J.F.: 'Physical properties of crystals' (Oxford University Press, Oxford, 1957)
8 BORN, M., and WOLF, E.: 'Principles of optics' (Pergamon Press, Oxford, 1980)
9 VENGSARKAR, A.M., THOMAS, D., ZIMMERMANN, B.D., and CLAUS, R.O.: 'Modal dependence of the photoelastic coefficient in multimode, step index optical fiber time domain systems', *IEEE J. Lightwave Technol.*, 1990, **2**, pp. 812–814
10 PAYNE, D.N., BARLOW, A.J., and RAMSKOV, J.J.: 'Development of low and high birefringence optical fibers', *IEEE J. Quantum Electron.*, 1982, **QE—18**, pp. 477–488
11 LANDAU, L.D., and LIFSHITZ, E.M.: 'Theory of elasticity' (Editorial Reverté, Barcelona, 1969)
12 SNYDER, A.W., and LOVE, J.D.: 'Optical waveguide theory' (Chapman and Hall, London, 1983, 2nd edn.)
13 DUGAS, J., PIERREJEAN, I., FARENC, J., and PEICHOT, J.P.: 'Birefringence and internal stress in polystyrene optical fibres', *Appl. Opt.*, 1994, **33**, pp. 3545–3548
14 KREVELEN, D.W.: 'Properties of polymers' (Elsevier, Amsterdam, 1990)
15 ISHIGURE, T., NIHEI, E., and KOIKE, Y.: 'Graded index polymer optical fibre for high speed data communication', *Appl. Opt.*, 1994, **33**, pp. 4261–4266
16 Mitsubishi Rayon Co., Ltd., Eska POFs
17 PAPP, A., and HARMS, H.: 'Polarisation optics of index-gradient optical waveguide fibers', *Appl. Opt.*, 1975, **14**, pp. 2406–2411